PCCP

Accepted Manuscript

This article can be cited before page numbers have been issued, to do this please use: L. Jia, C. M. Pedersen, Y. Qiao, T. Deng, P. Zuo, W. Ge, Z. Qin, X. Hou and Y. Wang, *Phys. Chem. Chem. Phys.*, 2015, DOI: 10.1039/C5CP02169C.

View Article Online
DOI: 10.1039/C5CP02169C

Glucosamine condensation catalyzed by 1-ethyl-3-methylimidazolium acetate: mechanistic insight from NMR spectroscopy

Lingyu Jia,[ab] Christian Marcus Pedersen,[c] Yan Qiao,[d] Tiansheng Deng,[a] Pingping Zuo,[d] Wenzhi Ge,[ab] Zhangfeng Qin,[d] Xianglin Hou,*[a] and Yingxiong Wang*[a]

[a] The Biorefinery Research and Engineering Center, Institute of Coal Chemistry, Chinese Academy of Sciences, Taiyuan, People's Republic of China.
E-mail: houxl@sxicc.ac.cn, wangyx@sxicc.ac.cn; Fax: +86 351 4041153; Tel: +86 351 4049501

[b] Graduate University of Chinese Academy of Sciences, Beijing, People's Republic of China

[c] Department of Chemistry, University of Copenhagen, Universitetsparken 5, DK-2100 Copenhagen Ø, Denmark

[d] State Key Laboratory of Coal Conversion, Institute of Coal Chemistry, Chinese Academy of Sciences, Taiyuan, People's Republic of China

Abstract

The basic ionic liquid 1-ethyl-3-methylimidazolium acetate ($[C_2C_1Im][OAc]$) could efficiently catalyze the conversion of 2-amino-2-deoxy-D-glucose ($GlcNH_2$) into deoxyfructosazine (DOF) and fructosazine (FZ). Mechanistic investigation by NMR studies disclosed that $[C_2C_1Im][OAc]$, exhibiting strong hydrogen bonding basicity, could coordinate with the hydroxyl and amino groups of $GlcNH_2$ *via* the promotion of hydrogen bonding in bifunctional activation of substrate and further catalyzing products formation, based on which a plausible reaction pathway involved in this homogeneous base-catalyzed reaction was proposed. Hydrogen bonding as an activation force, therefore, is responsible for the remarkable selectivity and rate enhancement observed.

Introduction

Concerns about global warming and energy security have directed researchers' focus on the use of biomass as alternative feedstocks to fossil resources for a variety of chemicals and fuels.[1-4] Chitin biomass, being the second most abundant class of

View Article Online
DOI: 10.1039/C5CP02169C

biopolymers (after the cellulose) on earth with an estimated global production of around 1×10^{10} tons each year, has attracted considerable attention as a sustainable and cost-effective organic nitrogen resource.[5-10] However, strategies for the utilization of biologically or chemically fixed nitrogen has not been fully exploited. The most abundant amino sugar, 2-amino-2-deoxy-D-glucose ($GlcNH_2$), as the monomer unit of polysaccharide chitosan, has an underestimated but remarkable potential for the production of renewable, value-added chemicals, especially N-containing compounds with potential pharmacological and biological activities (Scheme 1).[11-13] Direct conversion of $GlcNH_2$ into high valued chemicals bearing nitrogen in high yields is therefore a topic of increasing interest.

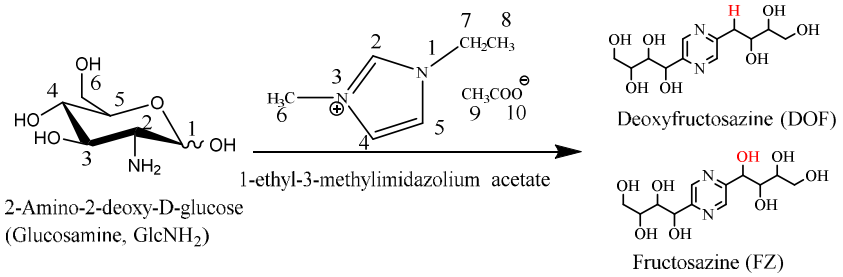

Scheme 1 A one-pot dehydration process to convert $GlcNH_2$ into DOF and FZ promoted by the basic imidazolium ionic liquid $[C_2C_1Im][OAc]$.

A major driving force for the development of ionic liquids (ILs) is the desire for greener chemical synthesis, which has aroused great interests both in academia and industry. ILs are often found to be a "greener" alternative to volatile organic solvents, and to have better properties than conventional solvents.[14-16] Efforts have been devoted to explore the dissolution mechanism of cellulose in ILs.[17-20] However, applications involving ILs are far beyond being just convenient "alternative" solvents, and thus numerous investigations are to explore their potential as effective catalysts for chemical reations.[10,19,21-27] The acidic and neutral ILs have been well recognized and successfully applied in many organocatalysis.[21-27] However, the basic ILs for the carbohydrates conversions were scarcely studied. 1-Ethyl-3-methylimidazolium acetate, $[C_2C_1Im][OAc]$ (Scheme 1), has emerged as one of the most promising candidates for performing chemical reactions in the context of Green Chemical

View Article Online
DOI: 10.1039/C5CP02169C

synthesis due to its non-toxicity and biodegradability.[16,18,19] More importantly, $[C_2C_1Im][OAc]$ with strong hydrogen bond basicity has been widely introduced as more environmentally benign reaction medium for the homogeneous physical or chemical modification of the polysaccharide with high efficiency.[18,19,21,28-31] Although $[C_2C_1Im][OAc]$ display high activity, to our knowledge there have been no reports of the use of $[C_2C_1Im][OAc]$ as catalysts for the conversion of chitin biomass. Another interesting effect of using ILs is the change in reaction mechanism/pathway which might occur and hence led to changes in product formation, yields and ratios.[32-34] Despite the ongoing wide interest in ILs, the nature of the catalyst-substrate interactions and the mechanism of *in situ* catalytic reaction pathways using basic ILs is not fully understood and only sporadically investigated.

It is reported that the main contribution to the carbohydrates–ILs interaction energy comes from favorable hydrogen bonding interactions between hydroxyl groups of carbohydrates and the cation or anion of the ILs.[18,28-31,35] Studies have additionally shown that the catalytic efficiency of [Bmim][OAc] predominantly stemmed from hydrogen bonding interactions, which are considered as the key intermediate state for further conversion.[32] The catalyst and substrate binding *via* the promotion of hydrogen bonding is the key point for this remarkable catalytic performance. Thus, ILs with specific hydrogen-bond donor/acceptor groups should enhance the ability of ILs to interact with the substrate, which favor ILs-substrate interactions and hence activation. These observations suggest that $[C_2C_1Im][OAc]$ could specifically coordinate with the hydroxyl and amino groups on $GlcNH_2$ due to its strong hydrogen bonding basicity. Our earlier investigations resulted in the development of [Bmim]OH as a dual solvent-catalyst for the synthesis of nitrogen heterocycles from bio-based carbohydrate $GlcNH_2$.[13] Therefore, $[C_2C_1Im][OAc]$, similar to the [Bmim]OH, displaying strong basicity, may play the same role in catalyzing conversion of $GlcNH_2$ to pyrazine derivatives. Herein, we report using $[C_2C_1Im][OAc]$ as the reaction medium to produce deoxyfructosazine (DOF) and fructosazine (FZ) from $GlcNH_2$

View Article Online
DOI: 10.1039/C5CP02169C

with high selectivity and rate enhancement in a single step. However, it is unclear how $[C_2C_1Im][OAc]$ catalyze biomass transformations. The modes of action of $[C_2C_1Im][OAc]$ on chitin biomass degradation need to be elucidated in order to develop and improve the catalysis process. To better understand the underlying mechanism of catalysis by $[C_2C_1Im][OAc]$ at a molecular level, we turned to NMR spectroscopy, which has been widely employed to characterize biomass conversion processes.[7,36] Hydrogen bonding interactions of $[C_2C_1Im][OAc]$, which were responsible for the selective conversion of $GlcNH_2$ *via* homogeneous catalysis, were elucidated for the first time at a molecular level.

Results and discussion

An initial NMR study showed that HCl-free $GlcNH_2$, when dissolved in DMSO-d_6, exhibit sufficient resolution to clearly identify distinct proton resonances of the hydroxyl and amino groups and carbon signals in the ^1H and ^{13}C NMR spectra, respectively (Fig. S1-S2, ESI†). The assignment of proton and carbon signals was obtained according to the literature and the 2D homo- or hetero- NMR spectra (Fig. S3-S5, ESI†).[11] Surprisingly, when a catalytic amount of $[C_2C_1Im][OAc]$ (molar ratio of $[C_2C_1Im][OAc]/GlcNH_2 = 0.1$) was added to the $GlcNH_2$/DMSO-d_6 solution, the peaks of the hydroxyl and amino groups quickly merged together and a new broad peak was observed in the ^1H NMR spectra (Fig. S6, ESI†). Interestingly, when the molar ratio of $[C_2C_1Im][OAc]/GlcNH_2$ was increased, the peak gradually moved downfield (Fig. 1). As it is known that traces of acid or base catalyzes proton exchange, the significant broadening of these proton resonance of the hydroxyl and amino groups is mainly due to the intermolecular proton exchange.[29,39] Presumably, the aromatic protons in the imidazolium cation, especially the most acidic H2, interacts with the oxygen or nitrogen atoms of the hydroxyl and amino groups and hence speed up the proton exchange rate. Lower field shift of the proton resonances of hydroxyls and amino was ascribed to the formation of hydrogen bonding between $GlcNH_2$ as hydrogen bonding donor and the CH_3COO^- anion as hydrogen bonding acceptor, whereas very little change in the chemical shifts was observed for the peaks

View Article Online
DOI: 10.1039/C5CP02169C

of methylene and methine in the $GlcNH_2$ backbone.[8,29] Previously, an "electrophile nucleophile dual activation" function of the ILs for catalysis through hydrogen bonding interactions has been proposed.[32] Thus, $[C_2C_1Im][OAc]$ could potentially provide bifunctional catalytic properties due to its specific structure, which can accept a proton and donate a proton at the same time *via* intermolecular hydrogen bonding interactions.[18] It is therefore believed that both the cation and anion of the $[C_2C_1Im][OAc]$ play a synergistical role in activation of the substrate during the catalysis. The specific binding interactions between $GlcNH_2$ and $[C_2C_1Im][OAc]$ were considered as a possible intermediate state for further isomerization in the condensation reactions leading to DOF and FZ.

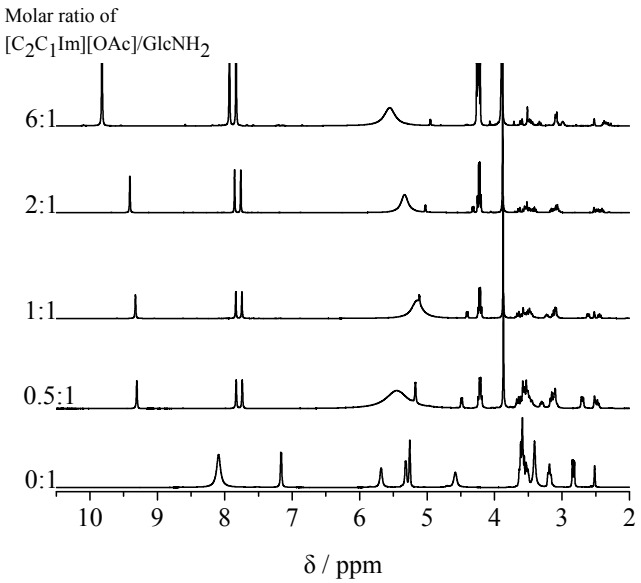

Fig. 1 The effect of molar ratios of $[C_2C_1Im][OAc]/GlcNH_2$ on the ^1H NMR spectra for $GlcNH_2$ in DMSO-d_6 solution (the chemical shift scale is in units of δ).

This assumption was further supported by the mutarotation behavior of the substrate. HCl-free $GlcNH_2$, when dissolved in the DMSO-d_6, was predominantly an α-anomer in the pyranose form (Fig. S1-S2, ESI†). Keeping the sample at room temperature for 3 days for equilibrium, the mutarotation between the α- and β-anomers of $GlcNH_2$ in DMSO-d_6 solution is still negligible according to the ^1H and ^{13}C NMR spectra (Fig. S7-S8, ESI†). However, in the presence of catalytic amounts of $[C_2C_1Im][OAc]$,

View Article Online
DOI: 10.1039/C5CP02169C

mutarotation to the equilibrium mixtures occurred rapidly (Fig. S9, ESI†). Besides, the relative intensity of peaks belonging to the β-anomer increased at the expense of the α-anomer when increasing the molar ratio of $[C_2C_1Im][OAc]/GlcNH_2$ (Fig. 2). An enlarged format of the area (δ = 50~100 ppm) highlighted by the dashed line was shown in the supporting information (Fig. S10, ESI†). As discussed above, specifically cooperative hydrogen bonding interactions presumably favor activation of the $GlcNH_2$, hence facilitating the interconversion of the α- and β-anomers.

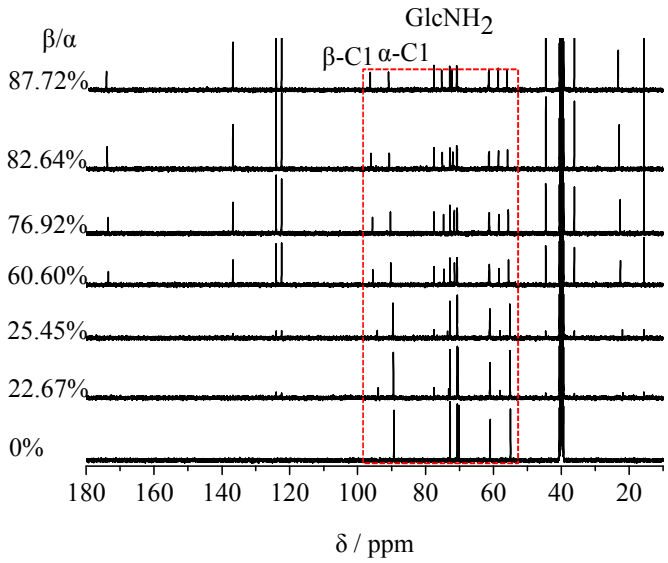

Fig. 2 The changes of β/α anomeric composition of $GlcNH_2$ calculated according to the integral area of β-H1/α-H2 in the ^1H NMR spectra (the chemical shift scale is in units of δ and molar ratio of $[C_2C_1Im][OAc]/GlcNH_2$ = 0:1, 0.1:1, 0.2:1, 0.5:1, 0.6:1, 0.9:1, 1:1 from below to top).

Compared with the imidazolium cations bearing weaker hydrogen bonding acceptors, the ILs anions, displaying highest hydrogen bonding basicity, tend to form strong hydrogen bonding interactions with the substrate.[19] Therefore, the obtained results may support a hypothesis that the basic CH_3COO^- anion could promote the proton transfer and further facilitate mutarotation of $GlcNH_2$ in such catalytic system.[16,19] The relatively small CH_3COO^- anion, as good hydrogen bonding acceptor and exhibiting great capability of forming hydrogen bonding, favors attacking hydrogen

View Article Online
DOI: 10.1039/C5CP02169C

atoms of the more activated anomeric hydroxyl, thus leading to mutarotation. $GlcNH_2$ is usually in the pyranose forms, however, its conversion to DOF and FZ is proposed to proceed *via* the straight-chain form.[13,34] It was shown that simple aldehydes can be converted through the CH_3COO^- anion within the ILs according to the pathway depicted in Fig. 3, giving a semiacetal-type structure. Consequently, it is reasonable to deduce that $GlcNH_2$-$[C_2C_1Im][OAc]$ coordination *via* hydrogen bonding is promoting the formation of the acyclic form for $GlcNH_2$ and facilitating the activation of nitrogen electron pair as a nucleophile, which then undergo further intermolecular nucleophilic cyclization and dehydration to produce the six-membered heterocycle pyrazine derivatives, called DOF and FZ. In summary, these results clearly indicate that the hydrogen bonding is formed between the hydroxyls and amino of $GlcNH_2$ and $[C_2C_1Im][OAc]$.

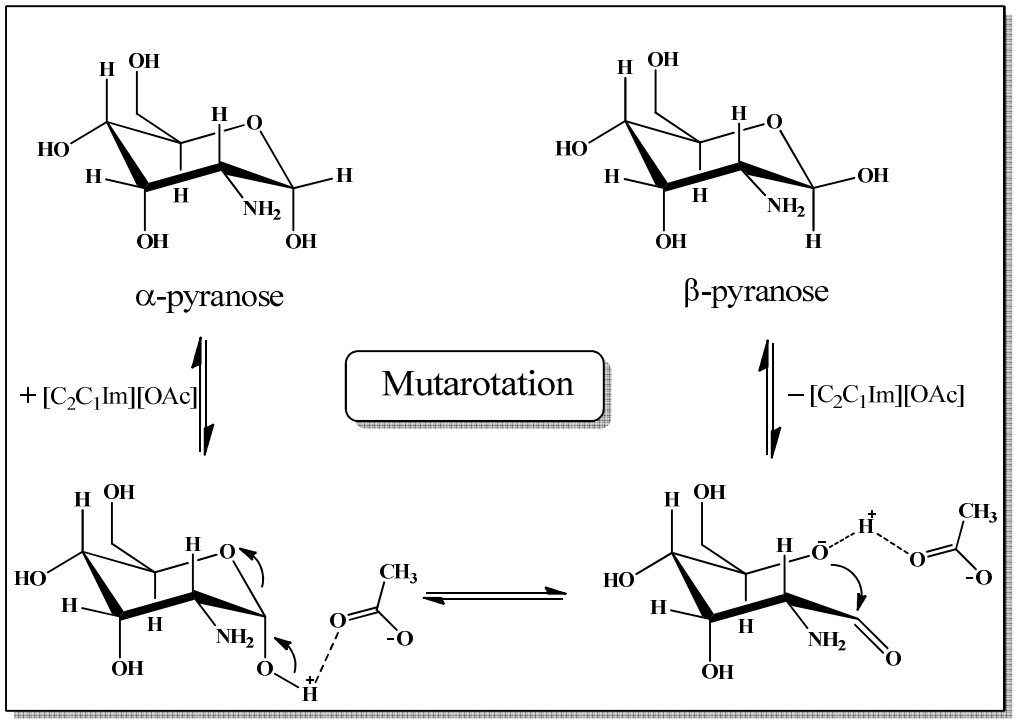

Fig. 3 Proposed $[C_2C_1Im][OAc]$ interaction with $GlcNH_2$ in DMSO. Acetate anion catalyze the mutarotation leading to interconversion of α- and β-pyranose anomers.

Furthermore, the formation of hydrogen bonding between $GlcNH_2$ and $[C_2C_1Im][OAc]$ is expected to affect carbon atoms around the the hydroxyls and amino groups.

View Article Online
DOI: 10.1039/C5CP02169C

Therefore, the ^{13}C NMR chemical shifts difference ($\Delta\delta$) values of the $GlcNH_2$ were employed to further support the above-mentioned suggestion. It was concluded from NMR spectra, in particular from ^{13}C NMR experiments, the CH_3COO^- anion, is much more involved in the interaction with the more acidic hemiacetal hydroxyl group in $GlcNH_2$ (C1-OH), which promote the ring opening and subsequent nucleophilic addition to give the products. The ^{13}C NMR chemical shifts and chemical shift difference ($\Delta\delta$) values for the above different cases are listed in Table S1 according to the numbering marked in Scheme 1. As the molar ratio of $[C_2C_1Im][OAc]/GlcNH_2$ increased, both the peaks of α-C1 and β-C1 markedly shift downfield compared with other carbons (indicated by the light-blue frame in Table S1). $[C_2C_1Im][OAc]$ might also interact with other accessible hydrogen atoms of the $GlcNH_2$ such as the hydroxyl groups at α-C4 or β-C3, leading to downfield shifts. These positions are, however, not directly involved in the condensation steps (Fig. 4).[29] Generally, DOF and FZ are obviously formed through an intermolecular nucleophilic addition reaction involving the activated carbonyl carbon (C1) and nitrogen electron pair as a nucleophile.[13] Thus, the observed obvious changes in the ^{13}C chemical shift of $GlcNH_2$ could confirm the specific coordination interactions between C1-OH of the $GlcNH_2$ and CH_3COO^- anion, and further explain the nucleophilic activation of $GlcNH_2$ by hydrogen bonding interactions. Activation of the nucleophile by CH_3COO^- anion through hydrogen bonding interactions during the catalysis has earlier been proposed.[32] It was therefore stated that the pronounced catalytic performance originated from an explicit hydrogen bond interactions between proton-acceptor sites of $[C_2C_1Im][OAc]$ anion and proton-donor hydroxyl and amino groups of the $GlcNH_2$ in catalyzing DOF and FZ formation. In addition, to guarantee a completely homogeneous synthesis pathway, the addition of solvent like DMSO is necessary. Our experimental results showed that addition of DMSO as solvent was weakly coordinating and could facilitate the solvation between $GlcNH_2$ and $[C_2C_1Im][OAc]$ without impairing the performance of the $[C_2C_1Im][OAc]$.[40,41]

View Article Online
DOI: 10.1039/C5CP02169C

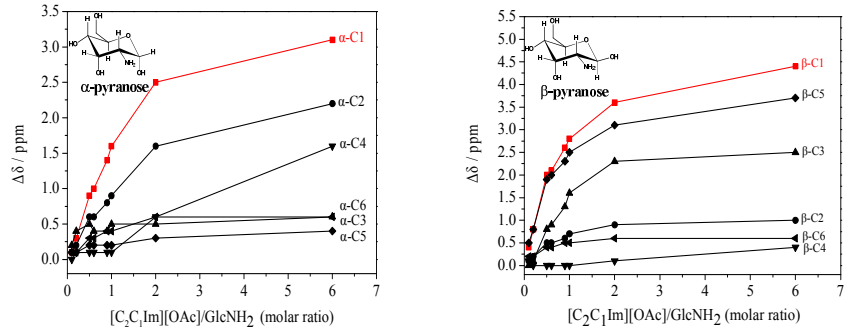

Fig. 4 Trend of the chemical shift difference of carbons in ^{13}C NMR of $GlcNH_2$ (α- and β-anomers) with increasing $[C_2C_1Im][OAc]$ concentration ($\Delta\delta=\delta_{obs}-\delta_0$, the chemical shift scale is in units of δ).

The above results clearly confirmed that hydrogen bonding is formed between $GlcNH_2$ and $[C_2C_1Im][OAc]$, supporting the existence of intermolecular contacts and the bifunctional activation of $GlcNH_2$. However, the interaction sites of $[C_2C_1Im][OAc]$ during catalysis still remain unknown. Thus, the effect of $GlcNH_2$ concentration on the ^1H and ^{13}C chemical shifts of $[C_2C_1Im][OAc]$ was investigated as well to elucidate the interaction sites on the ILs during catalysis. The ^1H and ^{13}C NMR chemical shifts and Δδ values for the above different cases are listed in Table S2 and S3. For the chemical shifts of the protons in the imidazolium ring, it was observed that the chemical shift of H2 is more sensitive to the addition of $GlcNH_2$, showing a marked upfield shift (indicated by the light-green frame in Table S2).[28-31,42] However, negligible changes were observed in methyl and ethyl protons of the cation and anion as the concentration of $GlcNH_2$ increased (Fig. 5a). The possible explanation is that relatively weak intermolecular hydrogen bonding was formed between oxygen or nitrogen atoms of $GlcNH_2$ and the most acidic H2 in the imidazolium ring while disrupting the interionic hydrogen bonding network in ILs, leading to an upfield shift.[19,29] Moreover, ^{13}C chemical shifts of $[C_2C_1Im][OAc]$ have been investigated as well and the results were shown in Fig. 5b. The carbonyl (C=O) of the CH_3COO^- anion moved downfield significantly, indicating that the strong hydrogen bonding was formed between CH_3COO^- anions and hydroxyl and amino groups of $GlcNH_2$.[28,29] In addition, the peaks of C2 showed a pronounced upfield change, while negligible

View Article Online
DOI: 10.1039/C5CP02169C

changes were observed for the other carbon atoms on the cation as the concentration of $GlcNH_2$ increased, further indicating weaker hydrogen bonding between the most acidic H2 of the imidazolium cation and $GlcNH_2$ was formed leading to upfield change of C2. More interestingly, a significant decrease in the value of the chemical shift of C9 (CH_3COO^-) was also found (indicated by the light-red frame in Table S3). This clearly indicates strong hydrogen bond interactions between the carboxyl and hydroxyl and amino groups were formed, which led to the increase of electron density around the C9 nucleus and thus a upfield shift of its ^{13}C NMR signal. A similar phenomenon of ILs has also been observed by Zhang et al. for cellulose dissolved in $[C_2C_1Im][OAc]$.[29] Both ^1H and ^{13}C NMR spectra confirmed that the catalytic efficiency of the $[C_2C_1Im][OAc]$ it does not solely due to the CH_3COO^- anions, and the imidazolium cation also play a key role in the molecular interactions during catalysis. For $GlcNH_2$ conversion, therefore, $[C_2C_1Im][OAc]$ was favored.

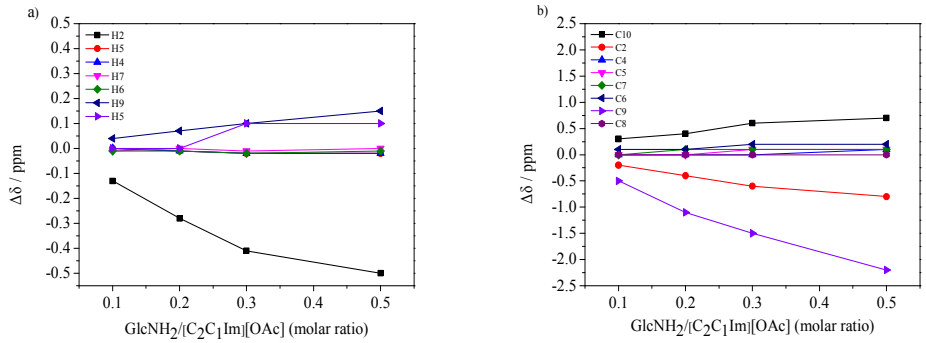

Fig. 5 Changes of proton (a) and carbon (b) chemical shift difference in $[C_2C_1Im][OAc]$ with increasing $GlcNH_2$ in DMSO-d_6 ($\Delta\delta = \Delta\delta_{obs} - \Delta\delta_{pure}$, the chemical shift scale is in units of δ).

The findings clearly indicated that hydrogen bonding is formed between $GlcNH_2$ and $[C_2C_1Im][OAc]$, and this can account for the enhanced reactivities observed. Therefore, ^1H-^1H homonuclear NOE spectra were recorded in order to provide straightforward and complementary information about these interactions.[28,36] As depicted in Fig. S11, a close contact can be visualized between the overlapped peak of $GlcNH_2$ hydroxyl and amino protons and the CH_3COO^- anions. Besides, a cross peak

View Article Online
DOI: 10.1039/C5CP02169C

between H2 imidazolium ring proton and the active hydrogen groups of the $GlcNH_2$ was also found. Hydrogen bonding interactions, therefore, do exist between $GlcNH_2$ and $[C_2C_1Im][OAc]$ during catalysis process and this is probably the main driving force for the catalysis. As expected, variations in spin-lattice relaxation time (T1) can provide information about the dynamics of ILs and present quantitative data regarding their interactions with the solute.[17] Thus, spin-lattice relaxation time of the ^1H nuclei of $[C_2C_1Im][OAc]$ was therefore studied. As presented in Table 1, there were only slight variations in the relaxation time of the protons in the cations of the $[C_2C_1Im][OAc]$ as a function of the $GlcNH_2$ content. Conversely, the relaxation parameters of the CH_3COO^- anion (H9) were strongly influenced by the presence of $GlcNH_2$ (see the light-purple frame in Table 1). The change in the longitudinal relaxation time of the CH_3COO^- anion with the increasing $GlcNH_2$ concentration was vastly larger than those expected due to the variation of the solution viscosity alone. The T1 value of the CH_3COO^- anion (H9), on the other hand, decreased drastically. This agreed with the conclusions presented earlier, and provided further evidence regarding the formation of hydrogen bonding between the CH_3COO^- anions and the carbohydrate hydroxyl and amino groups.[17,43]

Table 1. Spin-Lattice Relaxation Time T1 (s) of the corresponding protons of the $[C_2C_1Im][OAc]$ in the neat ILs (0:1) and the carbohydrate/IL solutions (molar ratio = 1:1 and 2:1)

	H-2	H-5	H-4	H-7	H-6	H-9	H-8
0:1	1.169	3.010	3.064	1.337	1.473	2.933	1.916
1:1	1.337	3.317	3.340	1.347	1.443	1.881	1.990
2:1	1.306	2.638	2.700	1.123	1.175	1.643	1.682

Based on the above results, both 1D and 2D NMR spectra clearly confirmed that hydrogen bonding is the main driving force for the $GlcNH_2$ catalytic conversion in $[C_2C_1Im][OAc]$. Therefore, if all the hydroxyls and amino of $GlcNH_2$ were acetylated, there would be no chance for the formation of hydrogen bonding between the substrate and $[C_2C_1Im][OAc]$. To verify the conclusion stated above, analogous measurements were carried out on solutions of D-glucosamine pentaacetate, a

View Article Online
DOI: 10.1039/C5CP02169C

molecule lacking hydrogen bond donors comparable to that of $GlcNH_2$. As expected, there was only a minor variation in the signals of D-glucosamine pentaacetate in the presence of $[C_2C_1Im][OAc]$ both in the ^1H and ^{13}C NMR spectra, presumably due to the inability of D-glucosamine pentaacetate as an inferior hydrogen bonding donor to form intermediate state for further dehydration (Fig. 6).[17,29] Thus, an "electrophile nucleophile dual activation" process of $[C_2C_1Im][OAc]$ for catalysis through hydrogen bonding interactions cannot proceed. Actually, experimental results further prove our conjecture, showing that no products were formed even at high temperature (80 °C) for 2 hours (Fig. S12, ESI†). Therefore, in contrast to D-glucosamine pentaacetate, $GlcNH_2$, as better hydrogen bonding donor, tend to form strong interactions with $[C_2C_1Im][OAc]$, i.e. hydrogen bonding is a major driving force for the catalytic conversion of $GlcNH_2$ in $[C_2C_1Im][OAc]$.

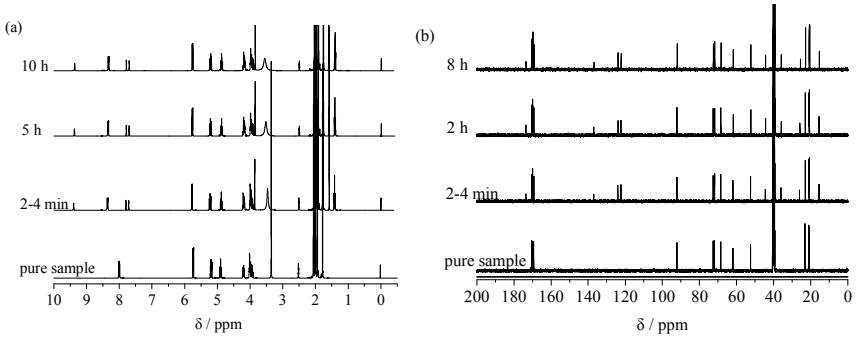

Fig. 6 Effect of $[C_2C_1Im][OAc]$ on the signal changes of glucosamine pentaacetate both in the ^1H (a) and ^{13}C NMR (b) spectra (the chemical shift scale is in units of δ and molar ratio of $[C_2C_1Im][OAc]$/glucosamine pentaacetate = 0.5:1).

Although the importance of hydrogen bonding was justified by above-mentioned experiments, it is not known if this catalytic mechanism would really work in the real system. To understand the catalytic mechanism in the real system, an *in situ* NMR study with $GlcNH_2$ as substrate and $[C_2C_1Im][OAc]$ as catalyst was carried out in DMSO-d_6 at 60 °C (Fig. 7). As it can be seen the peaks of hydroxyl and amino protons of $GlcNH_2$ overlapped each other and changed into one unresolved broad peak. The overlapped peaks gradually shifted upfield since hydrogen bonding will be

View Article Online
DOI: 10.1039/C5CP02169C

broken as temperature increased, which were in accordance with previous research.[17,29] Moreover, our ^{1}H NMR studies shows that the ratio between the anomers changes significantly. Thus, these behaviors were similar to the results observed at ambient temperature and directly indicated that relatively strong hydrogen bonding interactions indeed exist even at higher temperature. Additionally, when increasing the reaction temperature and time, DOF and FZ were gradually formed (indicated by the light-green frame in Fig. 7).[44-46]

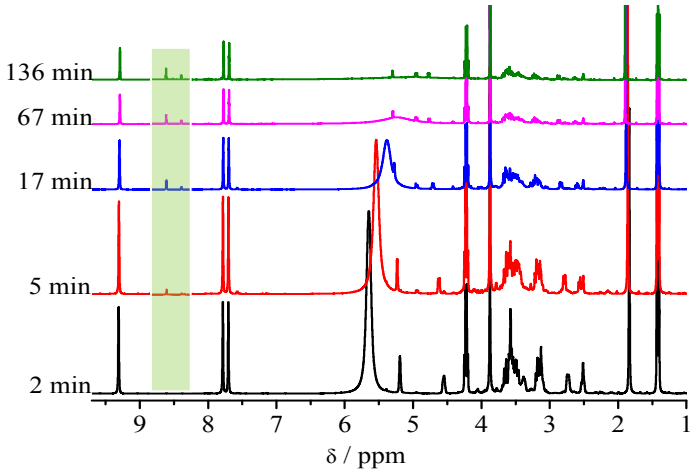

Fig. 7 The time-progression stack of *in situ* ^{1}H NMR spectra of $GlcNH_2$ catalyzed by $[C_2C_1Im][OAc]$ in DMSO-d_6 solution at 60 °C (the chemical shift scale is in units of δ).

Based on above NMR spectral study, a plausible reaction pathway was proposed in order to elucidate the catalysis process for the formation of the two pyrazine derivatives with this specific $[C_2C_1Im][OAc]$. The surprising finding was that the mechanism of catalysis highlighted the importance of not only the electrophilic nucleophilic dual activation through hydrogen bonding interactions but also activation of the nitrogen lone pair electrons by $[C_2C_1Im][OAc]$, facilitating further nucleophilic addition reactions and leading to the formation of DOF and FZ. Studies on interaction sites of $[C_2C_1Im][OAc]$ by ^{13}C NMR have found that the carbonyl (C=O) of the CH_3COO^- anion moved downfield significantly. CH_3COO^- anion, therefore, was proposed to interact with hydrogen atoms of the more activated anomeric hydroxyl of the sugar to give a complex, which increases the concentration of the open chain aldose form of the sugar.[13,34] In addition, based on the shift changes in ^{13}C NMR, as

View Article Online
DOI: 10.1039/C5CP02169C

the molar ratio of $[C_2C_1Im][OAc]/GlcNH_2$ increased, both the peaks of α-C1 and β-C1 markedly shift downfield compared with other carbons, clearly demonstrating that the specific interaction between the more acidic hemiacetal hydroxyl group in $GlcNH_2$ (C1-OH) and the CH_3COO^- anion, thus facilitating the formation of open chain aldose form of the amino sugars. Next, intermolecular nucleophilic addition involving the activated carbonyl carbon (C1) and nitrogen electron pair as a nucleophile affords the six-membered heterocycle, an intermediate typically called dihydropyrazine (Schiff Bases), in which an dehydrogenation (oxidative) process leading to FZ – this process is facilitated by the presence of hydrogen peroxide and simultaneously a dehydration and isomerization (electrolytic rearrangement) to give DOF.[13,45,47] Interestingly, activation of nitrogen electron pair by $[C_2C_1Im][OAc]$ is also a key factor determining the formation of pyrazine derivatives due to condensation reaction involving the aldehyde and nitrogen electron pair acts as a nucleophile. For comparison and to provide evidence for the nucleophilicity of amino-nitrogen, the reaction of GlcNAc was studied under similar conditions. GlcNAc as the starting material, 0% yield of DOF and FZ was obtained in the presence of catalytic amounts of $[C_2C_1Im][OAc]$ at relatively high temperature (Fig. S13, ESI†). This result was surprising given the high catalytic activity of $[C_2C_1Im][OAc]$ in the dehydration of $GlcNH_2$. This difference may be due to the presence of basic nitrogen electron pair within $GlcNH_2$ and its absence in GlcNAc. In recent literatures, GlcNAc was known to yield 3-acetamido-5-acetylfuran, in which nucleophilic attack by a hydroxyl group affords the five membered heterocycle, presumably due to the single acetylation of amino group in the GlcNAc, decreasing the nucleophilic activities of nitrogen atom and thus inhibiting the nucleophilic addition.[5,6,9] Thus, amino group containing an active lone pair of electrons on the electronegative nitrogen atom favors the nucleophilic addition process. Therefore, it is indicating that the CH_3COO^- anion enhanced nucleophilic ability of the nitrogen electron pair and the imidazolium cation improved the electrophilic ability of the aldehyde by forming intermolecular hydrogen bonds, which were the main driving force for this catalytic reaction. The proposed reaction mechanism was presented in Scheme 2. Although, some clues concerning the mechanism have been obtained, more detailed studies are currently underway in our research group.

View Article Online
DOI: 10.1039/C5CP02169C

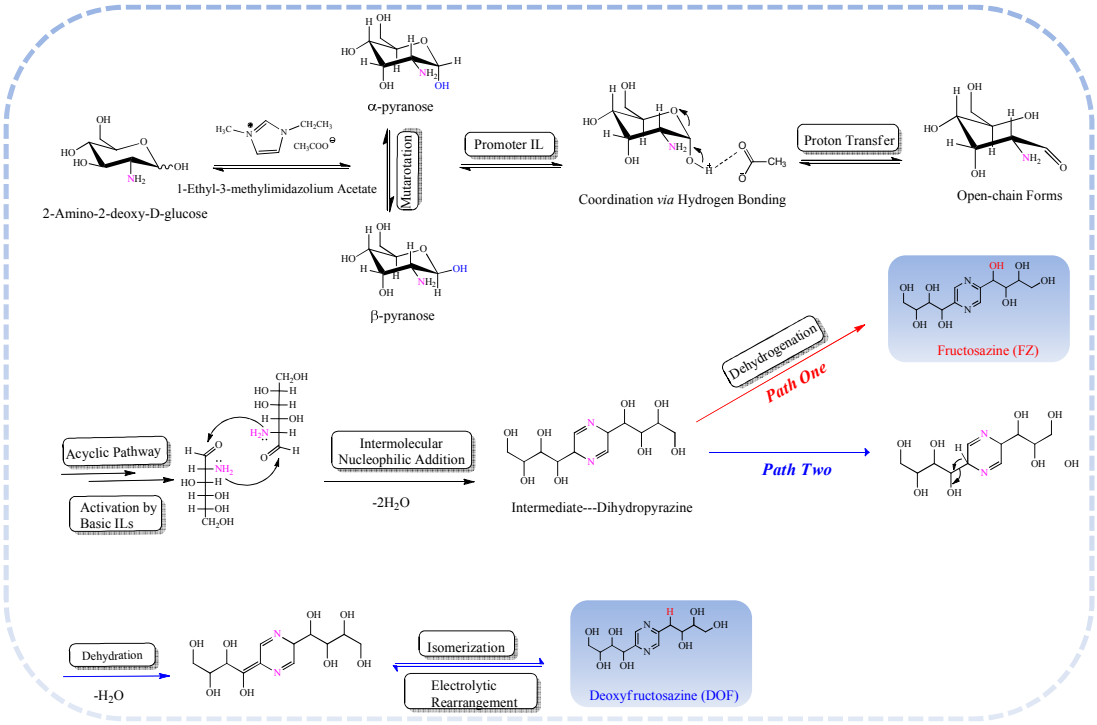

Scheme 2. Proposed reaction pathways for the formation of fructosazine (path one in red) and deoxyfructosazine (path two in blue) from $GlcNH_2$.

To explore the kinetic behavior of the self-condensation of $GlcNH_2$, investigation on a variety of reaction parameters was performed in the real system. In the blank experiment, i.e. in the absence of $[C_2C_1Im][OAc]$, no products were detected at 80 °C with different reaction times (Fig. S14, ESI†), confirming that DMSO is inactive for the production of DOF and FZ, which was in accordance with the mechanistic studies above.[40,41] The presence of catalytic amounts of $[C_2C_1Im][OAc]$ could efficiently catalyze the condensation reaction of $GlcNH_2$ to obtain the DOF and FZ, which were qualitatively identified by ^1H NMR, ^{13}C NMR, ^1H-^1H COSY, and HSQC spectra (Fig. S15-S18, ESI†). As evident by Fig. 8, significant effects of reaction temperature and time on the substrate conversion (with black curves) and yields of products (with blue curves) were observed. As increasing the temperature from 60 to 100 °C, both substrate conversion (indicated by black arrow) and product yields (indicated by blue arrow) clearly enhanced. The yields of DOF and FZ, and $GlcNH_2$ conversion were quantitatively calculated by ^1H NMR spectroscopy using pyrazine as an internal standard.[48] The maximum yields of products were 37%, which was achieved at

View Article Online
DOI: 10.1039/C5CP02169C

100 °C after a reaction time of 90 min (Fig. 8). Isolated yields of the DOF and FZ were provided in Figure S19. In addition, an ESI-MS spectrum showed that there were mainly two molecular cations $(M+H)^+$ at m/z 305.15 and 321.15 g/mol, respectively, corresponding to $[M\ (DOF) + H]^+$ and $[M\ (FZ) + H]^+$ (Fig. S20, ESI†). On the other hand, a rapid darkening of the reaction solution from light yellow to brown was observed, when the reaction time was increased from 5 to 120 min (Fig. S21, ESI†). Soluble polymers were presumably formed during the reaction though it is difficult to confirm this by NMR spectroscopy. Typically, the condensation of $GlcNH_2$ to DOF and FZ is a complex multistep process with many possible pathways and side reactions.[49,50]

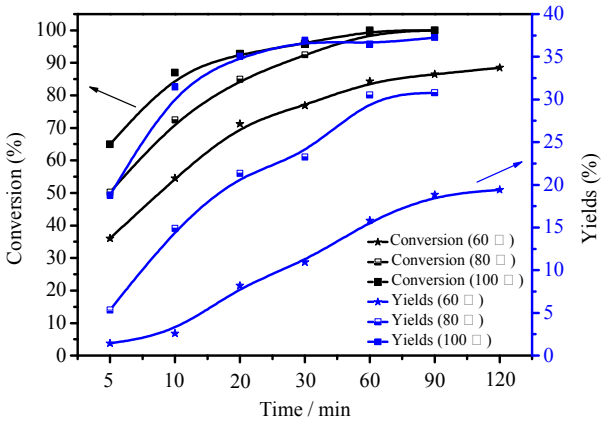

Fig. 8 $GlcNH_2$ conversion and product yields at different reaction time and temperature.

Conclusions

In summary, the detailed catalytic mechanism of $[C_2C_1Im][OAc]$ was elucidated *via* the investigation of the hydrogen bonding interactions between $[C_2C_1Im][OAc]$ and $GlcNH_2$ using NMR techniques. The CH_3COO^- anion was identified as the primary catalyst, while the cations of $[C_2C_1Im][OAc]$ worked synergistically to form hydrogen bonds, thus activating the substrate and facilitating the homogeneous base-catalyzed reaction. Our NMR data clearly demonstrated that the hydrogen bonding was formed between $GlcNH_2$ and $[C_2C_1Im][OAc]$, and suggest that this is the major driving force

View Article Online
DOI: 10.1039/C5CP02169C

for the catalytic reactions. $[C_2C_1Im][OAc]$, presented fascinating catalytic performance, could efficiently convert $GlcNH_2$ into DOF and FZ with high yields and selectivity. Based on NMR studies, a plausible reaction pathway was proposed. Consequently, understanding the catalytic nature of ILs will open up a new avenue for selective transformation of non-edible biomass into high value-added chemicals with potential industrial applications.

Experimental details

1.1 Materials

Practical grade D-glucosamine hydrochloride (designated as $GlcNH_2 \cdot HCl$, white crystalline powder) was obtained from Golden-Shell Biochemical Co. Ltd. HCl-free D-glucosamine sample was prepared by stirring with triethylamine and dichloromethane for 2-3 days until without crystalline solid. After stirring, samples were extracted by dichloromethane for 4-5 times to remove triethylamine hydrochloride as much as possible. $[C_2C_1Im][OAc]$ was purchased from Shanghai Cheng Jie Chemical Co. Ltd. DMSO-d_6 (99.9%, atom D) was supplied by Qingdao Teng long Microwave Technology Co. Ltd. Deuterium oxide (D_2O, 99.9% atom D) was supplied by Cambridge Isotope Laboratory. Dimethylsulfoxide (DMSO), pyrazine (internal standard) and all other chemicals (analytical grade) were purchased from Sinopharm Chemical Reagent Co. Ltd. All reagents were used without further purification.

1.2 General reaction procedures

The condensation reaction of $GlcNH_2$ was carried out in a round bottom flask that was heated in the oil-bath in the range from 60 °C to 100 °C with a continuous magnetic stirring and a condenser. Typically, 179.2 mg $GlcNH_2$ was added into desired 170.2 mg $[C_2C_1Im][OAc]$ (molar ratio 1:1) followed by the addition of 2 ml co-solvent of dimethylsulfoxide (DMSO). The reaction was vigorously stirred until a

View Article Online
DOI: 10.1039/C5CP02169C

transparent solution was formed. At different time intervals, 0.1 ml samples were taken, and quenched immediately with ice water bath for further analysis. For comparison, similar procedures were followed for $GlcNH_2$ condensation in pure DMSO in the absence of the $[C_2C_1Im][OAc]$ catalyst. Besides, similar reaction procedure was performed for N-acetyl-D-glucosamine (GlcNAc) and D-glucosamine pentaacetate as substrate at high temperature, respectively. The yields of DOF and FZ, as well as the $GlcNH_2$ conversion during the reaction, were quantitatively analyzed by ^1H NMR spectroscopy using pyrazine as internal standard substance. Pyrazine with concentration of 0.3 mg/ml in D_2O as standard solution was prepared and 0.1 ml of reaction mixture was mixed with 0.4 ml this standard solution to give the ^1H NMR sample. DOF and FZ yields were calculated as:

$$\text{Yield} = 2 \times \frac{moles\ of\ products}{moles\ of\ substrates} \times 100\%$$

1.3 NMR sample preparation

For observing the changes in ^{13}C chemical shifts of $GlcNH_2$ with increasing $[C_2C_1Im][OAc]$ concentrations, samples were prepared by adding different amounts of $[C_2C_1Im][OAc]$ into solutions of 0.5 ml DMSO-d_6 and 20 mg $GlcNH_2$. Ultrasonic treatment of the samples was applied to ensure complete dissolution of the substrates in the ILs prior to NMR analysis. Similarly, to analyze the effect of $GlcNH_2$ concentration on the proton and carbon chemical shifts of $[C_2C_1Im][OAc]$, samples were prepared by adding different weights of $GlcNH_2$ into the solution of 0.5 ml DMSO-d_6 and 20 mg $[C_2C_1Im][OAc]$ with constant stirring ($GlcNH_2$: $[C_2C_1Im][OAc]$ mass ratio: 0, 10, 20, 30, 50 wt%). Upon complete dissolution, samples were quickly transferred into 5 mm NMR tubes and measured by NMR. For comparison, samples were prepared by adding certain amounts of $[C_2C_1Im][OAc]$ into the solution 20 mg D-glucosamine pentaacetate and GlcNAc in 0.5 ml DMOS-d_6, respectively (the molar ratio of $[C_2C_1Im][OAc]$/glucosamine pentaacetate or GlcNAc = 0.5:1). Procedures for samples preparation were also used to acquire ^1H–^1H NOESY spectra.

View Article Online
DOI: 10.1039/C5CP02169C

1.4 *In situ* NMR sample preparation

Samples were prepared by adding 179 mg $GlcNH_2$ into desired 85 mg $[C_2C_1Im][OAc]$ (the molar ratio of $GlcNH_2/[C_2C_1Im][OAc]$ = 2:1) followed by the addition of 0.5 ml DMSO-d_6, which provided a field-frequency lock and NMR internal standards. After complete dissolution, the samples were transferred into 5 mm NMR tube. When the temperature inside the NMR spectrometer probe was stabilized at 60 ℃, the tube was immediately transferred to the NMR spectrometer. *In situ* ^{1}H NMR spectra were recorded at certain times during the experiment.

1.5 Characterization

The 1D and 2D NMR spectra were acquired on a Bruker AV-III 400 MHz NMR spectrometer (9.39 T) equipped with auto sampler. ^{1}H and ^{13}C NMR spectra were obtained at frequencies of 400.13 and 100.61 MHz, respectively. ^{1}H and ^{13}C NMR titration experiments were operated at room temperature with 16 scans and 500 scans, respectively. *In situ* ^{1}H NMR experiments were performed at 353 K. NOESY NMR experiments were carried out using standard library sequences with mixing times, τ_m, of 500 ms at room temperature. All spectra were acquired using DMSO-d_6 for field-frequency lock. Spin-lattice relaxation time (T1) measurement of the $[C_2C_1Im][OAc]$ protons was carried out at 298 K. The T1 values were measured by the inversion recovery pulse program (t1ir). Relaxation measurements were carried out with relaxation delays at least five times T1 and the instrument was carefully tuned, shimmed, and the 90 degree pulse calibrated before each measurement. The products were further qualitatively identified by the positive-ion ESI mass spectrum on a Bruker MicroTOF-Q III.

Acknowledgements

The authors would like to acknowledge the financial support from the Major State Basic Research Development Program of China (973 Program) (No. 2012CB215305)

View Article Online
DOI: 10.1039/C5CP02169C

and Natural Science Foundation of China (No. 21106172, 21403273). Yan Qiao thanks the Chinese Academy of Sciences (2013YC002) and the Youth Innovation Promotion Association of Chinese Academy of Sciences (2011137) for financial support. Christian Marcus Pedersen acknowledges the CAS President's International Fellowship Initiative (2015VMB052). Special thanks are given to Jennifer Hongyang Zhang and Jun Ren for their assistance during revision.

Notes and references

1 A. Corma, S. Iborra and A. Velty, *Chem. Rev.*, 2007, **107**, 2411-2502.

2 M. J. Climent, A. Corma and S. Iborra, *Green Chem.*, 2014, **16**, 516-547.

3 L. Xu, Y. Jiang, Q. Yao, Z. Han, Y. Zhang, Y. Fu, Q. Guo and G. W. Huber, *Green Chem.*, 2014, **17**, 1281-1290.

4 T. Deng, X. Cui, Y. Qi, Y. Wang, X. Hou and Y. Zhu, *Chem. Commun.,* 2012, **48**, 5494-5496.

5 X. Chen, S. L. Chew, F. M. Kerton and N. Yan, *Green Chem.*, 2014, **16**, 2204-2212.

6 K. W. Omari, L. Dodot and F. M. Kerton, *ChemSusChem*, 2012, **5**, 1767-1772.

7 Y. Wang, C. M. Pedersen, T. Deng, Y. Qiao and X. Hou, *Bioresour. Technol.*, 2013, **143**, 384-390.

8 Q. Chen, A. Xu, Z. Li, J. Wang and S. Zhang, *Green Chem.*, 2011, **13**, 3446-3452.

9 F. M. Kerton, Y. Liu; K. W. Omari, K. Hawboldt, *Green Chem.* 2013, **15**, 860-871.

10 M. W. Drover, K. W. Omari, J. N. Murphy and F. M. Kerton, *RSC Adv.,* 2012, **2**, 4642-4644.

11 Y. Ohmi, S. Nishimura and K. Ebitani, *ChemSusChem*, 2013, **6**, 2259-2262.

12 C. K. S. Pillai, W. Paul and C. P. Sharma, *Prog Polym Sci.*, 2009, **34**, 641-678.

13 L. Jia, Y. Wang, Y. Qiao, Y. Qi and X. Hou, *RSC Adv.*, 2014, **4**, 44253-44260.

14 R. Sheldon, *Chem. Commun.*, 2001, 2399-2407.

15 H. Olivier-Bourbigou, L. Magna and D. Morvan, *Appl Catal A-Gen.,* 2010, **373**, 1-56.

View Article Online
DOI: 10.1039/C5CP02169C

16 N. R. Dhumal, H. J. Kim and J. Kiefer, *J. Phys. Chem. A.*, 2009, **113**, 10397-10404.

17 R. C. Remsing, R. P. Swatloski, R. D. Rogers and G. Moyna, *Chem. Commun.*, 2006, 1271-1273.

18 T. Liebert and T. Heinze, *BioResources,* 2008, **3**, 576-601.

19 M. Brehm, H. Weber, A. S. Pensado, A. Stark and B. Kirchner, *Phys. Chem. Chem. Phys.,* 2012, **14**, 5030-5044.

20 M. E, Zakrzewska, E. Bogel-yukasik, R, Bogel-yukasik. Energy Fuels 2010, **24**, 737-745.

21 T. Welton, *Coord. Chem. Rev.*, 2004, **248**, 2459-2477.

22 A. C. Cole, J. L. Jensen, I. Ntai, K. L. T. Tran, K. J. Weaver, D. C. Forbes and J. H. Davis, Jr, *J. Am. Chem. Soc.,* 2002, **124**, 5962-5963.

23 A. S. Amarasekara, M. A. Hasan. *Tetrahedron Lett.,* 2014, **55**, 3319-3321.

24 A. S. Amarasekara, A. Razzaq. *Carbohydr. Res.*, 2014, **386**, 86-91.

25 J. Viell and W. Marquardt, *Appl. Spectrosc.*, 2012, **66**, 208-217.

26 J. Kiefer, K. Obert, A. Bosmann, T. Seeger, P. Wasserscheid and A. Leipertz, *Chemphyschem.*, 2008, **9**, 1317-1322.

27 M. Thomas, M. Brehm, O. Holloczki, Z. Kelemen, L. Nyulaszi, T. Pasinszki and B. Kirchner, *J Chem Phys*, 2014, **141**, 024510.

28 J. M. M. Araujo, A. B. Pereiro, J. N. Canongia Lopes, L. P. Rebelo and I. M. Marrucho, J. *Phys. chem. B.*, 2013, **117**, 4109-4120.

29 J. Zhang, H. Zhang, J. Wu, J. Zhang, J. He and and J. Xiang, *Phys. Chem. Chem. Phys.*, 2010, **12**, 1941-1947.

30 M. E. Ries, A. Radhi, A. S. Keating, O. Parker and T. Budtova, *Biomacromolecules*, 2014, **15**, 609-617.

31 P. A. Hunt, C. R. Ashworth and R. P. Matthews, Chem. Soc. Rev., 2015, **44**, 1257-1288.

View Article Online
DOI: 10.1039/C5CP02169C

32 A. K. Chakraborti and R. S. Roy, *J. Am. Chem. Soc.,* 2009, **131**, 6902-6903.

33 A. R. Hajipour and F. Rafiee, *J. Iran. Chem. Soc.*, 2009, **6**, 647-678.

34 E. A. Khokhlova, V. V. Kachala, V. P. Ananikov. *ChemSusChem* 2012, **5**, 783-789.

35 A. Pinkert, K. N. Marsh, S. S. Pang and M. P. Staiger, *Chem. Rev.*, 2009, **109**, 6712-6728.

36 V. P. Ananikov, *Chem. Rev.*, 2011, **111**, 418-454.

37 D. Horton, J. S. Jewell, K. D. Philips, *J. Org. Chem.*, 1966, **31**, 4022-4025.

38 X. Sun, Q. Tian, Z. Xue, Y. Zhang and T. Mu, *RSC Adv*. 2014, **4**, 30282-30291.

39 H. B. Zhao, J. E. Holladay, H. Brown and Z. C. Zhang, *Science*, 2007, **316**, 1597-1600.

40 J. M. Andanson, E. Bordes, J. Devémy, F. Leroux, A. A. H. Pádua and M. F. C. Gomes, *Green Chem.*, 2014, **16**, 2528-2538.

41 R. C. Remsing, Z. W. Liu, I. Sergeyev and G. Moyna, *J. Phys.Chem. B,* 2008, **112**, 7363-7369.

42 C. S. Lovell, A. Walker, R. A. Damion, A. Radhi, S. F. Tanner, T. Budtova and M. E. Ries, *Biomacromolecules*, 2010, **11**, 2927-2935.

43 N. Assa-Munt, J. Granot, R. W. Behling and D. R. Kearns, *Biochemistry* 1984, **23**, 944-955.

44 J. Rohovec, J. Kotek, J. A. Peters and T. Maschmeyer, *Eur. J. Org. Chem.,* 2001, **2001**, 3899-3901.

45 K. Sumoto, M. Irie, N. Mibu, S. Miyano, Y. Nakashima K. Watanabe and T. Yamaguchi, *Chem. Pharm. Bull.*, 1991, **39**, 792-794.

46 S. Wu, H. Fan, Q. Zhang, Y. Cheng, Q. Wang, G. Yang and B. Han, *Clean-Soil Air Water*, 2011, **39**, 572-576.

47 N. Kashige, T. Yamaguchi, N. Mishiro, H. Hanazono, F. Miake and K. Watanabe, *Biol. Pharm. Bull.,* 1995, **18**, 653-658.

48 T. Rundlöf, M. Mathiasson, S. Bekiroglu, B. Hakkarainen, T. Bowden and T. Arvidsson, *J. pharmaceut. biomed.*, 2010, **52**, 645-651.

View Article Online
DOI: 10.1039/C5CP02169C

49 H. Tsuchida, Hiromichi, M. Komoto, H. Kato and M. Fujimaki, *Agr. Biol. Chem.*, 1973, **37**, 2571-2578.

50 A. P. Zhu, J. B. Huang, A. Clark, R. Romero and H. R. Petty, *Carbohydr. Res.*, 2007, **342**, 2745-2749.